Surface-plasmon voltammetry using a gold grating

2010 J. Phys. D: Appl. Phys. 43 385301

(http://iopscience.iop.org/0022-3727/43/38/385301)

IOP PUBLISHING JOURNAL OF PHYSICS D: APPLIED PHYSICS

J. Phys. D: Appl. Phys. **43** (2010) 385301 (7pp) doi:10.1088/0022-3727/43/38/385301

Surface-plasmon voltammetry using a gold grating

M J Jory, P S Cann and J R Sambles

Electromagnetic Materials Group, School of Physics, Stocker Road, University of Exeter, Exeter EX4 4QL, UK

Received 14 April 2010, in final form 30 July 2010
Published 7 September 2010
Online at stacks.iop.org/JPhysD/43/385301

Abstract

Using a sensitive optical wavelength modulation technique the surface-plasmon excited on a gold grating surface immersed in sulfuric acid is studied at the same time as cyclic voltammetry is undertaken. Because of the optical sensitivity of the modulation technique significant optical effects are observed at potentials well below those at which any gross oxidation effects occur.

1. Introduction

The electrochemical response of the gold/electrolyte interface continues to be the subject of extensive research [1–13]. Cyclic voltammetry has been used to establish the current–voltage characteristics of the well-ordered surfaces associated with single-crystal electrodes [1, 2, 4, 6]. Both the oxidation/reduction processes occurring at high anodic potentials and the more subtle changes that occur within the double-layer region have been studied, see for example Hamelin *et al* [1]. Additionally, several techniques have been used in combination with cyclic voltammetry to gain further information regarding these processes including scanning-tunnelling microscopy (STM) [14–18], atomic-force microscopy (AFM) [19], the quartz crystal microblance (QCM) [20–22], reflectance studies [23], ellipsometry [24–27] and surface-plasmon resonance (SPR) studies [28–38]. It is SPR-electrochemistry, which has now been recognized as a new and powerful tool for exploring not just electrochemistry but also bioelectrochemistry [37–40], that is of interest in this work.

A surface-plasmon polariton (SPP) is a coupled electromagnetic wave/longitudinal charge density oscillation that may be excited along the interface between a metal and a dielectric. The associated enhanced optical fields decay exponentially away from the interface extending $\sim\lambda/10$ into the metal and $\sim\lambda$ into the dielectric (where λ is the optical wavelength, typically $\sim$400 nm in electrolyte.) Consequently, SPR-based techniques are sensitive to changes in the working electrode, the double-layer region and the charging of the diffuse layer [28–38].

The momentum of a SPP propagating along a metal/dielectric interface is greater than that of a grazing photon of the same frequency in the bulk dielectric. Consequently, it is not possible to optically excite SPR directly, it is necessary to enhance the in-plane momentum of the incident beam. Traditionally there are three configurations in which this momentum enhancement is achieved in order to study the electrochemical interface using SPR. The first two involve a prism of refractive index greater than that of the surrounding electrolyte. In one arrangement, the Otto geometry [41], the prism is set so that one face is separated from the working electrode surface (usually gold or silver in the visible) by $\sim 0.5\,\mu$m [28, 29]. Having passed through the prism, light striking the prism/electrolyte interface beyond the critical angle is totally internally reflected. However, an evanescent wave is also produced that extends into the transmitting medium tunnelling across the narrow electrolyte gap and exciting SPR on the working electrode surface. This configuration allows the use of bulk, highly ordered single-crystal working electrodes that are vital for studying fundamental, crystal-face sensitive, electrochemical processes using cyclic voltammetry [1]. However, this geometry has the disadvantages that, due to the small gap between prism and electrode, it is both difficult to fabricate and does not readily allow studies incorporating a flow of electrolyte as is often required in adlayer deposition, biosensing and/or cleaning of the electrode surface. It is because of the aforementioned reasons that the alternative Kretschmann–Raether prism [42] geometry is often used. Here an optically thin ($\sim$45 nm thick) layer of gold is evaporated onto one face of a high-index prism (or on a glass substrate which is index matched to a prism). Now beyond the prism/electrolyte critical angle light tunnels through the gold film and excites an SPR on the outer electrode surface. This Kretschmann–Raether geometry overcomes the small gap fabrication and 'trapped-electrolyte'

problems of the Otto system and is much better suited to biosensing applications where the use of well-ordered single-crystal electrodes is not so crucial [30, 33–40]. However, the optically thin metal film is very fragile and consequently does not allow extended electrochemical deposition cycles to be performed on the same electrode. In general, this geometry also necessitates the use of polycrystalline electrodes although there are exceptions [23].

The third geometry for SPR excitation is grating coupling [43]. The simplest example is a diffraction grating possessing a periodic surface with a well-specified groove depth and pitch. The translational invariance of the grating surface is broken in one direction by the grooves. This means that momentum may be added to, or subtracted from the x-component of the momentum of incoming photons. (The 'x-direction' is defined as parallel to the plane of the grating and perpendicular to the direction of the grooves.) Conservation of momentum in the x-direction gives [43]

$$n_{\mathrm{el}} k_0 \sin\theta_{\mathrm{i}} \pm mG = k_{\mathrm{SPP}}, \tag{1}$$

where n_{el} is the refractive index of the electrolyte, k_0 is the magnitude of the wavevector of the incident light in free-space, θ_{i} is the angle-of-incidence, $k_{\mathrm{SPP}} = k_0(\varepsilon_{\mathrm{metal}}\varepsilon_{\mathrm{el}}/(\varepsilon_{\mathrm{metal}} + \varepsilon_{\mathrm{el}}))^{1/2}$ is the SPP wavevector ($\varepsilon_{\mathrm{metal}}$ and $\varepsilon_{\mathrm{el}}$ being the real parts of the optical permittivities of the metal and electrolyte, respectively), m is an integer and $G = 2\pi/\lambda_{\mathrm{g}}$ is the magnitude of the grating wavevector (λ_{g} being the pitch of the grating grooves.) When equation (1) is satisfied an SPR may be excited on the grating surface directly from the dielectric half-space (i.e. the electrolyte) without the constraints placed on the thickness of the metal electrode or the electrolyte gap that are associated with the Kretschmann–Raether [42] and Otto [41] methods, respectively. As this grating configuration openly presents the entirety of a robust, bulk, working electrode to the electrolyte it may prove invaluable in the field of biosensing and opto-electrochemistry.

In this work we monitor the optical changes that occur at the electrochemical interface between a diffractive gold electrode and an acid electrolyte using an acousto-optic differential reflectivity detection technique [44]. This detection system allows the position of the SPR, in wavelength, to be continuously monitored as cyclic voltammetry is performed [45].

2. Experimental

2.1. Electrode preparation

A clean, fused-silica disc is spin-coated [46] with a photoresist layer. Using a standard interferographic method a diffraction grating of groove pitch 600 nm and groove depth 20 nm is manufactured in the photoresist. This groove pattern is then transferred to the underlying silica substrate by ion-beam etching using a low-pressure argon plasma. Full details of this method can be found elsewhere [47].

A gold film, at least 150 nm thick, is now evaporated onto the fused-silica diffraction grating. In order to improve adhesion between the gold and the silica, the bare grating is

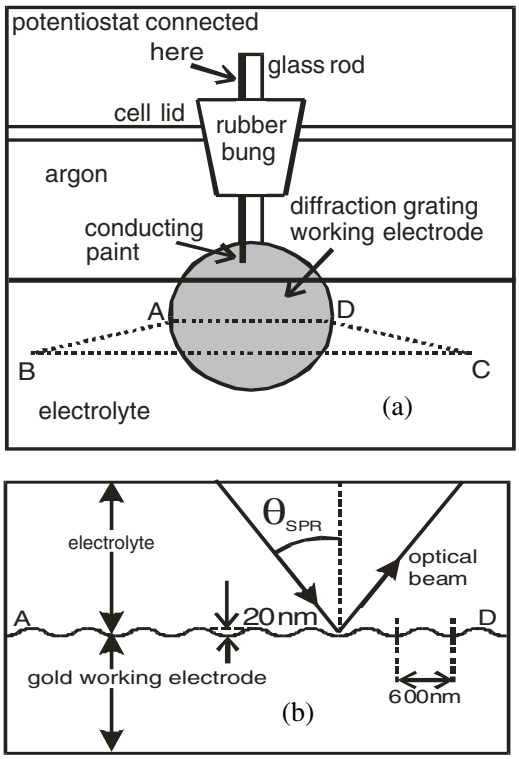

Figure 1. (a). Experimental arrangement. ABCD is the (horizontal) plane of incidence. The grating grooves lie perpendicular to ABCD; (b) experimental arrangement. In this work $\theta_{\mathrm{SPR}} = 14.3^{\circ}$.

first immersed in a solution of 0.01M dithiodipropionic acid in ethanol for 20 min. On removal from the solution the grating is allowed to dry in air and cleaned with chloroform-soaked cotton buds and lens tissue to remove the excess residue. The gold film is then deposited by evaporation in 10^{-6} Torr.

The gold-coated grating is now partially immersed in a 0.02M H_2SO_4 electrolyte (as shown in figure 1(a)) (This acid solution is prepared from 99.999% pure sulfuric acid and 18 MΩ cm conductivity de-ionized water.) The grating is orientated so that its grooves lie vertically. A 99.999% pure gold wire used as the counter electrode and a standard Ag/AgCl reference electrode complete the cell. (All potentials are quoted with respect to Ag/AgCl.) Before any electrochemical measurements are taken, the electrolyte is purged of oxygen, for a period of 1 h, by a continuous flow of argon gas. Cyclic voltammetry is then performed in the conventional way [48]. (A minimal argon flow through the electrolyte is maintained during all the measurements.)

2.2. Optical measurements

Light, whose wavelength has been selected from a white light source by an acousto-optic tuneable filter (AOTF) [49] is now directed through the electrolyte and onto the working electrode (i.e. the gold diffraction grating) at an incidence angle of 14.3° (figure 1(b)). The grating has previously been orientated so that the optical plane of incidence (ABCD in figure 1(a)) is horizontal and lies perpendicular to the groove direction. Sweeping the AOTF drive frequency from

63 to 125 MHz gives an optical wavelength scan from 775 to 425 nm. Using a photomultiplier tube (PMT) detector, the reflected intensity from the gold/electrolyte interface is monitored simultaneously. SPR excitation is observed as a minimum in the reflectivity at ∼660 nm [44]. A frequency modulation is now added to the AOTF carrier signal resulting in a wavelength modulation of the optical beam. This, in turn, causes the reflected intensity at the electrochemical interface to be modulated. Measuring the modulated output from the PMT detector with a lock-in amplifier (set to operate at the frequency of modulation) provides a direct measure of the differential reflectivity with respect to wavelength. The SPR minimum observed in the conventional reflectivity measurement now corresponds to a position of zero differential that sits on a steep linear background [44].

Having set the phase of the lock-in amplifier appropriately, a computer program is now used to lock the wavelength of the optical beam (by adjusting the AOTF carrier frequency) to the position of zero differential, i.e. the SPR position. With this system it is possible to measure the SPR position in wavelength to a precision of 0.0005 nm [44]. While continuing to monitor the SPR wavelength, the potential of the working electrode is swept between −500 and 850 mV at 10 mV s^{-1}. Thus, a direct measure of SPR position in wavelength is obtained versus time as cyclic voltammetry is performed. A full explanation of this acousto-optic SPR technique can be found elsewhere [44].

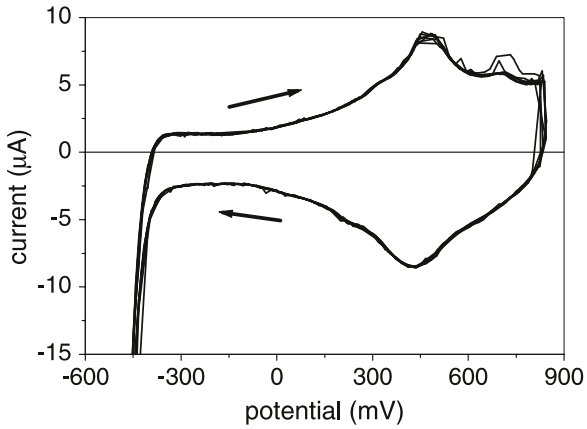

Figure 2. Cyclic voltammogram for a polycrystalline gold-diffraction grating electrode in 0.02M H_2SO_4 electrolyte. The potential is cycled between −500 and 850 mV at 10 mV s^{-1}.

3. Results and discussion

Figure 2 shows a cyclic voltammogram obtained on a gold-coated diffraction grating-working electrode. Hydrogen evolution occurs on the positive sweep up to about −400 mV after which double-layer charging occurs. There is then a major peak in the current at 475 mV corresponding to adsorption of sulfate ions. On the negative sweep sulfate desorption occurs at 420 mV with hydrogen evolution re-commencing at −380 mV. These data are consistent with the conventional response of a polycrystalline gold electrode in weak sulfuric acid [14, 36, 50, 51]. The periodic surface profile of the electrode (having a groove depth : pitch ratio = 0.03) appears to have no effect on the electrochemistry of the interface.

Figure 3 depicts electrode potential (solid line) and SPR position in wavelength (open circles) versus time. The SPR position clearly oscillates, as cyclic voltammetry is performed, with resonance wavelength amplitude 0.97 nm. These electrochemically induced changes in SPR position may also be considered as relative changes in SPP wavevector (as is also shown in figure 3) allowing ready comparison with the work of Abeles *et al* [32].

Figure 4 shows both current and SPR position versus potential. At the beginning of the upward potential sweep the SPP wavevector increases at a rate of $\sim 3.0 \times 10^{-7} (\Delta k_{spp}/k_0)\,mV^{-1}$ (or in terms of resonant optical wavelength 1.4×10^{-4} nm mV^{-1}). As the potential increases through 0 mV the gradient of the curve rises steadily until a point of inflection is reached at 480 mV (very close to the sulfate adsorption current peak position) with gradient $4.2 \times 10^{-6} (\Delta k_{spp}/k_0)\,mV^{-1}$ (2.4×10^{-3} nm mV^{-1}). At the end of the positive potential sweep the curve has gradient $2.3 \times 10^{-6} (\Delta k_{spp}/k_0)\,mV^{-1}$ (1.1×10^{-3} nm mV^{-1}). The second branch of the curve, recorded upon reversing the direction of potential sweep, has a similar shape to the first, this time with the point of inflection occurring at 440 mV, again very close to the negative peak in current corresponding to sulfate desorption. We also note that the SPR position recorded at the most negative potential (−550 mV) rises systematically with each cycle. At this minimal potential $\Delta k_{spp}/k_0$ has a value of 0.01×10^{-3} (662.14 nm SPR wavelength) recorded at the start of the measurements. By the end of the eighth cycle this value has risen to 0.14×10^{-3} (662.20 nm). This behaviour is

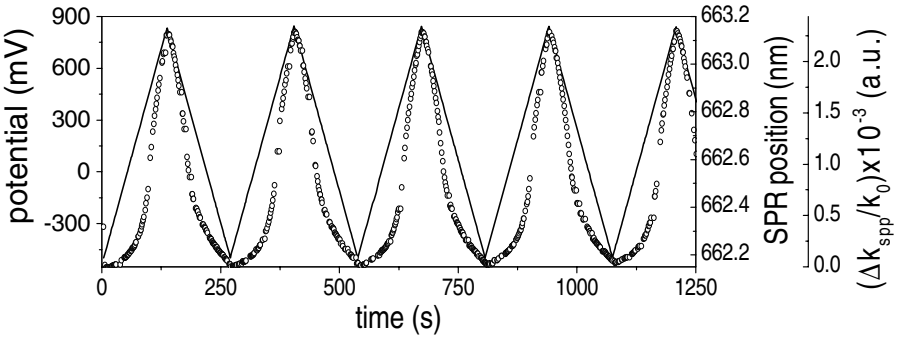

Figure 3. Electrode potential (solid line) and SPR position in wavelength (open circles) versus time. SPR position may also be considered as relative change in SPP wavevector (far right axis).

not observed at the positive potential end of the cycles where a $\Delta k_{spp}/k_0$ value of $2.27(\pm 0.01) \times 10^{-3}(663.143(\pm 0.005)$ nm) is always recorded. It is clear that the faradaic currents (with peak values $-60(\pm 5)$ μA at potentials beyond -295 mV) due to hydrogen evolution have surprisingly little direct effect on the SPP position.

These data agree well with that found by other authors on similar systems where the rate of change in SPR position with respect to potential is seen to increase as the electrode becomes more anodic, especially when anion adsorption occurs [30–32, 51, 52]. Here, we are able to monitor the SPR position continuously as cyclic voltammetry is performed and therefore are able to observe the hysteresis in the optical response of the interface. Our optical data are also in very good agreement with the changes in electrode weight monitored using a QCM for the gold/H_2SO_4 interface [22]. Other studies have shown that the electrode resistivity [53] exhibits a similarly asymmetric response.

Having noted that points of inflection in the SPR/potential curve agree well with the positions of current peaks it is logical to explore the differential of the SPR position with respect to time. Figure 5 shows a comparison between $(\partial/\partial t)(\Delta k_{spp}/k_0) = (\Delta k_{spp}/k_0)'$ (open circles) and current (solid line) versus time. There is good agreement between the two curves. Again we note that the large negative peak in current due to hydrogen evolution barely affects the SPR data.

The same data are shown in figure 6 but this time versus potential. Here there is a clear correlation between the time differential of the optical response (open circles) and the cyclic voltammogram (solid line). Current–voltage characteristics and the time differential SPR response have previously been compared by Iwasaki *et al* [34] who measured the change in SPR *angle* as a function of electrode potential for the *prism*-based Kretschmann–Raether system. However, they were unable to obtain such detailed data especially for potentials below the onset of anion adsorption. The sulfate adsorption and desorption peaks are clearly seen in our optical data. This correlation between $(\Delta k_{spp}/k_0)'$ and the current ($=\partial Q/\partial t$ where Q is charge) implies that the shift in SPP wavevector is, to a first approximation, proportional to charge. However, there appears to be an almost constant negative offset to the time differential SPR data for upward sweeping data before 365 mV and a similar positive offset for the downward sweep below 450 mV. This indicates that there is an almost abrupt change in either the optical nature of the surface or the electrical nature of the surface due to the absorption and desorption of the sulfate ions (although on the upward sweep the change is at a lower voltage than the 480 mV absorption peak). This would not be too surprising.

We now compare the optical data acquired for electrode potentials beyond -300 mV (the open circles in figure 7) with the computer-modelled response of a capacitor (185 μF) and resistor (30 kΩ) in series (solid line). At these potentials, the current measurements obtained using conventional cyclic voltammetry are dominated by faradaic currents (i.e. hydrogen evolution as mentioned above). However, it is clear that the SPR responds only to the underlying capacitor-like charging of the double layer. (It should be noted that for the purposes of this comparison, a slight negative offset (that is observed in both the electrical and optical data in figure 6) has been removed from the optical data in figure 7. We tentatively attribute this offset to low levels of dissolved oxygen or some other impurity in the electrolyte and/or hydrogen evolution at highly electroactive adatom sites.)

Figure 8 shows the SPP wavevector response (averaged over eight potential cycles) versus relative charge (charge being calculated by integrating current for potentials

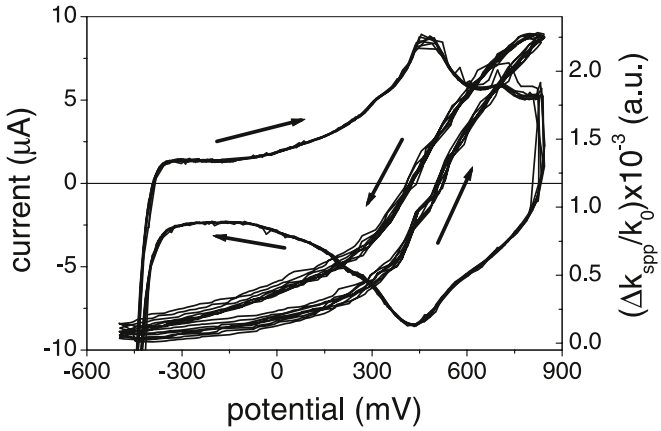

Figure 4. Cyclic voltammogram (left axis), as shown in figure 2, compared with relative change in SPP wavevector (right axis). The arrows indicate the potential sweep direction with respect to the SPP data.

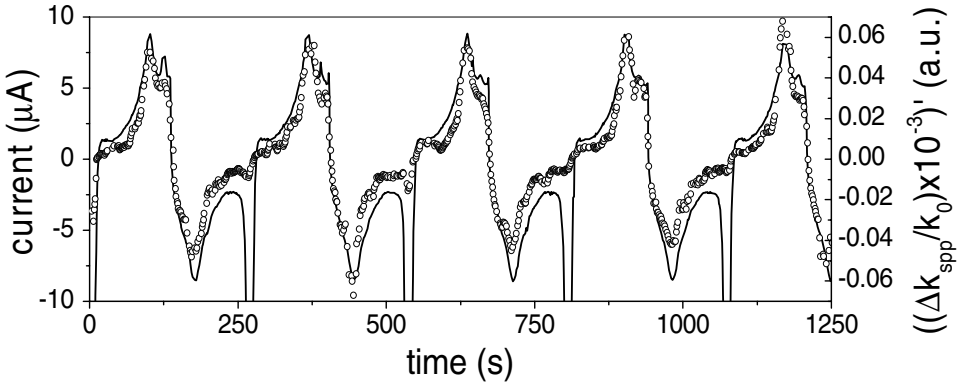

Figure 5. Time dependence of current (solid line) compared with that of the differential of the relative change in SPP wavevector with respect to time (circles).

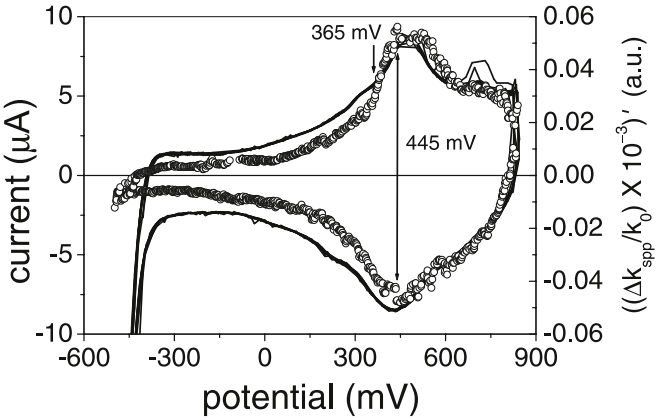

Figure 6. Cyclic voltammogram (solid line), as shown in figure 2, compared with the differential of the relative change in SPP wavevector with respect to time (circles).

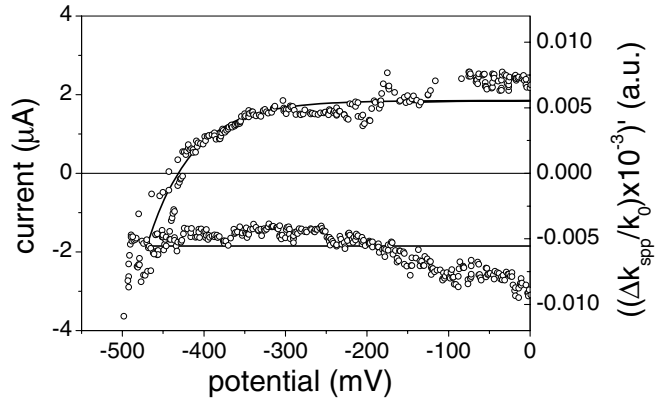

Figure 7. Computer-modelled current-potential response of a capacitor (185 μF) and resistor (30 kΩ) in series (line). Differential of the relative change in SPP wavevector with respect to time (circles).

above −310 mV). Initially, the SPR position (circles) increases at $(2.93 \pm 0.02) \times 10^{-6}\,\mu\mathrm{C}^{-1}$ as charge builds up on the electrode (arrow A in figure 8). (This rate is calculated by fitting a straight line to the data as shown in the figure.) Upon passing ∼170 μC (∼365 mV) the gradient changes quickly to a value of $(6.33 \pm 0.01) \times 10^{-6}\,\mu\mathrm{C}^{-1}$ that is maintained until 273 μC (∼500 mV) (arrows B and C). After this point a gradient of $(5.34 \pm 0.04) \times 10^{-6}\,\mu\mathrm{C}^{-1}$ is maintained (arrow D) until the end of the positive sweep (850 mV). The average SPR response for the negative potential sweep is also shown (crosses). Initially the SPR position decreases at a rate of $(5.18 \pm 0.02) \times 10^{-6}\,\mu\mathrm{C}^{-1}$ (arrow E) and this value is maintained until the charge drops to ∼210 μC (445 mV). For the rest of the potential cycle below 333 mV a gradient of $(-2.92 \pm 0.01) \times 10^{-6}\,\mu\mathrm{C}^{-1}$ (arrow F) is recorded (the opposite of the charge build-up gradient). (Again the solid lines represent linear fits to the data.) An increase in SPR-sensitivity to charging of the electrode has previously been observed [32] and attributed to the restructuring of the double layer and/or the onset of anion adsorption upon reaching the point of zero charge [31, 32]. The SPP wavevector response as a function of charge recorded in this work could be interpreted as indicating that anion adsorption is a two stage process, while desorption

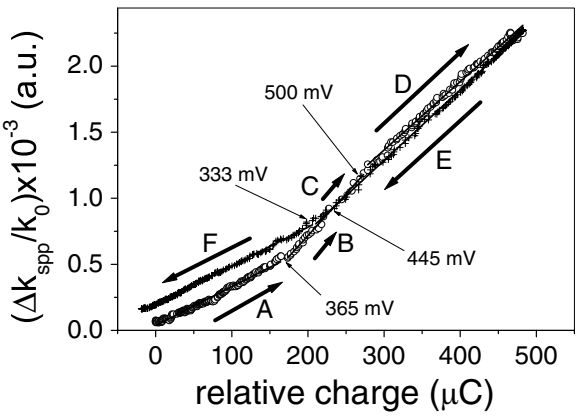

Figure 8. Relative change in SPP wavevector (averaged over 8 potential cycles) versus relative charge. The circles and crosses correspond to data acquired during the positive and negative going potential sweeps, respectively. Linear fits to the data are also shown (solid lines).

occurs in a single step. Moreover, the fact that the experimental data in figure 8 are multiple-valued (i.e. more than one value of $(\Delta k_{\mathrm{spp}}/k_0)$ for a given value of relative charge) suggests that the SPR is sensitive not only to the density of ions and water molecules in the ionic double layer but also to the double-layer structure.

It has been shown that the application of a potential across the gold/acid interface results in modification of the optical response of the metal, the double layer and the diffuse layer [23, 32]. The low frequency fields applied during cyclic voltammetry are typically screened within one atomic layer of the electrode surface [23, 32]. Forstmann *et al* [54] have shown that non-local optics must be used to accurately model the optical reflectivity response (known as the electroreflectance [55]) of a gold electrode in both the visible and ultra-violet. However, in this study the maximum photon energy used is 1.87 eV (equivalent to a wavelength of 662.15 nm). At such low photon energies the electroreflectance effect makes little contribution to the reflectivity of the interface with the predicted response using local and non-local optics being in good agreement [23, 54]. Furthermore, Abeles *et al* have shown that changes in the metal electrode predominantly contribute to changes in the imaginary part of the SPP wavevector and do not affect the real part [32]. As described above, the differential-detection technique used here only monitors the position, in wavelength, of the SPR—i.e. changes in the *real* part of the SPP wavevector—and so is insensitive to changes due to the electroreflectance effect. This, along with the good agreement between our data and QCM studies (that are insensitive to charging of the metal) of the same system [22] lead us to conclude that changes in SPR position are due to charging of the double and diffuse layer, anion adsorption and/or restructuring of the electrode surface. For the 0.02M electrolyte used in this work the double and diffuse layers combined have a thickness of no more than 2.15 nm [48], approximately 0.003 of an optical wavelength in the electrolyte. Consequently, we now model the optical response of the electrochemical interface by the addition of an isotropic over-layer with thickness $d = 2.15$ nm and optical permittivity

$\varepsilon_{\text{overlayer}}$. Here, the modified SPP wavevector becomes $k_{\text{SPP}}^{\text{mod}}$ where [56]

$$k_{\text{SPP}}^{\text{mod}} = k_{\text{SPP}} + \Delta k \tag{2}$$

with

$$\Delta k = k_0 \left(\frac{\varepsilon_{\text{overlayer}} - \varepsilon_{\text{el}}}{\varepsilon_{\text{overlayer}}} \right) \left(\frac{\varepsilon_{\text{metal}} \varepsilon_{\text{el}}}{\varepsilon_{\text{metal}} + \varepsilon_{\text{el}}} \right)^2 \times \left(\frac{\varepsilon_{\text{overlayer}} - \varepsilon_{\text{metal}}}{\varepsilon_{\text{el}} - \varepsilon_{\text{metal}}} \right) (-\varepsilon_{\text{metal}} \varepsilon_{\text{el}})^{-\frac{1}{2}} \left(\frac{2\pi d}{\lambda} \right). \tag{3}$$

As the ionic concentration of the double layer increases the local optical permittivity will increase above that of the bulk electrolyte resulting in a modification of the SPR position. If the bulk electrolyte is assumed to have an optical permittivity of 1.778 (refractive index 1.333) then the maximum shift in the SPP wavevector of $\Delta k/k_0 = 2.36 \times 10^{-3}$ (see figure 8) requires an over-layer permittivity of 2.04 (refractive index 1.428). Assuming that, to a first approximation, optical permittivity is proportional to density [57] then this is equivalent to an increase in ion concentration within the interfacial region of 14.7% (2.04/1.778 = 1.147) compared with that in the bulk.

4. Conclusions and future work

This work demonstrates that real time cyclic SPR voltammetry can be performed on polycrystalline-metal diffraction grating electrodes. The periodic surface profile of the electrode gives the momentum enhancement required to allow the SPR to be excited along the electrochemical interface but does not appear to affect the voltammetric response of the system. Using an acousto-optic differential-detection technique, the SPR position, in wavelength, is readily monitored as cyclic voltammetry is performed.

In the double-layer charging region the SPR response is found to correlate strongly with charge. This is most clearly illustrated by plotting SPR position (in terms of relative change in wavevector) as a function of relative charge. The differential-detection system used here allows the resonant optical wavelength to be monitored to a precision of 0.0005 nm [44]. This is equivalent to a sensitivity of $\sim 8 \times 10^{-4}$ of a sulfate ion monolayer. By optimizing the grating pitch and the refractive index contrast between the electro-deposited material and the bulk electrolyte it should be possible to improve this sensitivity by at least an order of magnitude.

Alternatively, the time differential of the SPR position may be plotted as a function of electrode potential thereby producing an 'optical voltammogram'. This has provided a detailed comparison between the electrochemical and optical responses of the gold/acid interface over the *entire* double-layer region.

As a first step, a simple theory has been used to model the electrochemical double layer as an isotropic over-layer having a thickness of 2.15 nm. Maximum SPR shift, observed when the electrode is covered by a complete anion monolayer, would require a double and diffuse-layer refractive index of 1.43. This implies a 14.7% increase in ion concentration compared with that of the bulk electrolyte.

The wavelength at which the SPR is excited along the electrode surface may be selected by tuning the incident angle of the optical beam. Thus, the optical response of a chosen electrode/electrolyte combination could be characterized across the visible spectrum. However, with higher-energy photons as the optical probe it may become necessary to use non-local optics theory to provide a satisfactory model of the electrochemical interface.

It is clear that the evolution of hydrogen at the cathodic end of the potential cycles has very little effect on the SPR position. However, the SPP does seem to be sensitive to the resulting changes in surface structure of the electrode. It is well established that the groove profile of a metallic diffraction grating can be characterized by fitting angle-dependent reflectivity data (acquired using a monochromatic optical beam) to Chandezon theory [58]. Characterizing the diffraction grating groove profile in this way, before and after the electrode has been subjected to cycles in potential, may provide an elegant means of monitoring the electrochemically induced changes in surface structure. Furthermore, comparison of the SPR response (at the cathodic end of the potential cycles) with the theoretical current-potential response of a simple capacitor/resistor network indicates that the SPP continues to respond to the underlying double-layer charging and electrode-surface restructuring processes even when gas-evolution is occurring. Studying this aspect of the SPR electrochemical response as a function of electrolyte concentration (thereby changing the resistance and capacitance of the double layer) may provide further insight into this phenomenon.

Having a thickness of 150 nm, these diffractive electrodes are far more robust than the traditional, optically thin (<100 nm thick), planar films used in the Kretschmann–Raether technique. In addition, silica diffraction gratings can be replicated in plastic readily and cheaply [59]. Consequently, this diffraction grating electrode arrangement is well-suited to biosensor systems where it may be desirable to electrochemically control the binding strength of a particular antigen [60].

Atom etching a grating directly into a bulk *single-crystal* electrode would provide, for the first time, a means of studying single-crystals via surface-plasmon excitation in a configuration that overcomes the dielectric tunnel barrier problem particular to the Otto geometry. Alternatively, the photoresist development process and/or the atom etch could be stopped before the photoresist layer has been completely removed so as to leave a periodic array of photoresist ridges on the electrode. Each ridge would then be separated from its nearest neighbours by an area of planar single-crystal metal. This will allow SPR studies of specific, well-defined single-crystal faces via diffraction from the photoresist ridges. Further, it would be possible to electrochemically deposit metal adlayers between these ridges. The optical response of a periodic array of metal adlayers could then be explored by simply dissolving the photoresist. By depositing an electro-chromic material on a diffractive electrode it may also be possible to create electrochemically tuneable photonic band-gaps.

Finally, combining the optical detection technique and cyclic voltammetry used here with an electrochemical QCM [22] may provide a further means of distinguishing between electrode processes.

Acknowledgments

The authors gratefully acknowledge the help of Mr D J Jarvis who prepared the gold films and the EPSRC for financial support.

References

[1] Hamelin A 1996 *J. Electroanal. Chem.* **407** 1
Hamelin A and Martins A M 1996 *J. Electroanal. Chem.* **407** 13
[2] Hamelin A, Stoicoviciu L, Edens G J, Gao X and Weaver M J 1994 *J. Electroanal. Chem.* **365** 47
[3] Hutton R S and Williams D E 1994 *J. Am. Chem. Soc.* **116** 3453
[4] Pajkossy T 1997 *Solid State Ion.* **94** 123
[5] Burke L D, Collins J A, Horgan M A, Hurley L M and O'Mullane A P 2000 *Electrochim. Acta* **45** 4127
[6] Silva F and Martins A 1998 *Electrochim. Acta* **44** 919
[7] Dutkiewicz E and Skoluda P 1991 *J. Electroanal. Chem.* **301** 247
[8] Burke L D and O'Leary W A 1989 *J. Appl. Electrochem.* **19** 758
[9] Lovrecek B, Moslavac K and Matic D J 1981 *Electrochim. Acta* **26** 1087
[10] Desilvestro J and Weaver M J 1986 *J. Electroanal. Chem.* **209** 377
[11] Horanyi G and Rizmayer E M 1984 *J. Electroanal. Chem.* **165** 279
[12] Burke L D and O'Mullane A P 2000 *J. Solid State Electrochem.* **4** 285
[13] Shi Z, Lipkowski J, Gamboa M, Zelenay P and Wiekowski A 1994 *J. Electroanal. Chem.* **366** 317
[14] Schneeweiss M A and Kolb D M 1997 *Solid State Ion.* **94** 171
[15] Gómez J, VasQuez L, Baro A M, Perdriel C L and Arvia A J 1989 *Electrochim. Acta* **34** 619
[16] Dakkouri A S 1997 *Solid State Ion.* **94** 99
[17] Trevor D J, Chidsey C E D and Loiacono D N 1989 *Phys. Rev. Lett.* **62** 929
[18] Vazquez L, Bartolome A, Baro A M, Alonso C, Salvarezza R C and Arvia A J 1989 *Surf. Sci.* **215** 171
[19] Manne S, Massie J, Elings V B, Hansma P K and Gewirth A A 1991 *J. Vac. Sci. Technol.* B **9** 950
[20] Gordon J S and Johnson D C 1994 *J. Electroanal. Chem.* **365** 267
[21] Tsionsky V, Daikhin L and Gileadi E 1996 *J. Electrochem. Soc.* **143** 2240
[22] Watanabe M, Uchida H and Ikeda N 1995 *J. Electroanal. Chem.* **380** 255
[23] Kolb D M 1988 *Spectroelectrochemistry* ed R J Gale (New York: Plenum Press) p 87
[24] Stedman M 1970 *The Symp. Faraday Soc.* **4** 1
[25] Abeles F and Lopez-Rios T 1980 *Surf. Sci.* **96** 32
[26] Sirohi R S and Genshaw M A 1969 *J. Electrochem. Soc.* **116** 910
[27] Horkans J, Cahan B D and Yeager E 1974 *Surf. Sci.* **46** 1
[28] Otto A 1980 *Surf. Sci.* **101** 99
[29] Tadjeddine A, Kolb D M and Kotz R 1980 *Surf. Sci.* **101** 277
[30] Gordon II J G and Ernst S 1980 *Surf. Sci.* **101** 499
[31] Kotz R, Kolb D M and Sass J K 1977 *Surf. Sci.* **69** 359
[32] Abeles F, Lopez-Rios T and Tadjeddine A 1975 *Solid State Commun.* **16** 843
[33] Jung C C, Saban S B, Yee S S and Darling R B 1996 *Sensors Actuators B—Chem.* **32** 143
[34] Iwasaki Y, Horiuchi T and Niwa O 2001 *Anal. Chem.* **73** 1595
[35] Iwasaki Y, Horiuchi T, Morita M and Niwa O 1997 *Electroanalysis* **9** 1239
[36] Chao F, Costa M and Tadjeddine A 1977 *J. Physique (Paris) Coll.* C **5** 97
[37] Zhang N, Schweiss R, Zong Y and Knoll W 2007 *Electrochim. Acta* **52** 2869
[38] Jakob T and Knoll W 2003 *J. Electroanal. Chem.* **543** 51
[39] Schlereth D 1999 *J. Electroanal. Chem.* **464** 198
[40] Heaton R J, Peterson A W and Giorgiadis R M 2001 *Proc. Natl Acad. Sci.* **98** 3701
[41] Otto A 1968 *Z. Phys.* **216** 398
[42] Kretschmann E and Raether H 1968 *Z. Naturf.* a **23** 2135
[43] Sambles J R, Bradberry G W and Yang F 1991 *Contemp. Phys.* **32** 173
[44] Jory M J, Bradberry G W, Cann P S and Sambles J R 1995 *Meas. Sci. Technol.* **6** 1193
[45] Jory M J, Bradberry G W, Cann P S and Sambles J R 1996 *Sensors Actuators* B **35** 197
[46] Vukusic P, Sambles J R and Wright J D 1992 *J. Mater. Chem.* **2** 1105
[47] Hutley M C 1982 *Diffraction Gratings* (London: Academic) p 95
[48] Brett C M A and Brett A M O 1993 *Electrochemistry Principles, Methods, and Applications A* (Oxford: Oxford University Press) p 48
[49] Gass P A and Sambles J R 1991 *Opt. Lett.* **16** 429
[50] Jusys Z and Bruckenstein S 1998 *Electrochem. Solid State Lett.* **1** 74
[51] Peuckert M, Coenen F P and Bonzel H P 1984 *Surf. Sci.* **141** 515
[52] Dzhavakhidze P G, Kornyshev A A, Tadjeddine A and Urbakh M I 1989 *Electrochim. Acta* **34** 1677
[53] Hansen W N 1980 *Surf. Sci.* **101** 109
[54] Forstmann F, Kempa K and Kolb D M 1983 *J. Electroanal. Chem.* **150** 241
[55] McIntyre J D E 1973 *Advances in Electrochemistry and Electrochemical Engineering* vol 9, ed R H Muller (New York: Wiley) p 61
[56] Pockrand I 1978 *Surf. Sci.* **72** 577
[57] Hecht E 1987 *Optics* 2nd edn (London: Addison-Wesley) p 111
[58] Chandezon J and Dupuis M T 1982 *J. Opt. Soc. Am.* **72** 839
[59] Bryan-Brown G P, Jory M C, Elston S J and Sambles J R 1993 *J. Mod. Opt.* **40** 959
[60] Toda K, Tsuboi M, Sekiya N, Ikeda M and Yoshioka K I 2002 *Anal. Chim. Acta* **463** 219